nature neuroscience

Ghrelin controls hippocampal spine synapse density and memory performance

Sabrina Diano[1,9], Susan A Farr[2,3], Stephen C Benoit[4], Ewan C McNay[5], Ivaldo da Silva[1], Balazs Horvath[1], F Spencer Gaskin[2,3], Naoko Nonaka[2,3], Laura B Jaeger[2,3], William A Banks[2,3], John E Morley[2,3], Shirly Pinto[6], Robert S Sherwin[5], Lin Xu[7], Kelvin A Yamada[7], Mark W Sleeman[8], Matthias H Tschöp[4] & Tamas L Horvath[1,9,10]

The gut hormone and neuropeptide ghrelin affects energy balance and growth hormone release through hypothalamic action that involves synaptic plasticity in the melanocortin system. Ghrelin binding is also present in other brain areas, including the telencephalon, where its function remains elusive. Here we report that circulating ghrelin enters the hippocampus and binds to neurons of the hippocampal formation, where it promotes dendritic spine synapse formation and generation of long-term potentiation. These ghrelin-induced synaptic changes are paralleled by enhanced spatial learning and memory. Targeted disruption of the gene that encodes ghrelin resulted in decreased numbers of spine synapses in the CA1 region and impaired performance of mice in behavioral memory testing, both of which were rapidly reversed by ghrelin administration. Our observations reveal an endogenous function of ghrelin that links metabolic control with higher brain functions and suggest novel therapeutic strategies to enhance learning and memory processes.

Ghrelin, the endogenous ligand of growth hormone secretagogue (GHS) receptors, has been shown to influence pituitary hormone secretion, appetite, metabolism, gastrointestinal function and the cardiovascular and immune systems[1–5]. Synthetic GHS receptor (GHS-R) agonists and antagonists are available and have been proposed as treatments for growth hormone deficiency or metabolic disorders, such as obesity and cachexia[3–5]. Based on the many functions that have emerged regarding endogenous ghrelin, an increasing number of other potential uses for GHS-R agonists and antagonists can be anticipated. The finding that GHS-R expression[6,7] and ghrelin binding sites are present outside of the hypothalamus (in the cerebral cortex[8], for example) raises the possibility that peripheral administration of ghrelin or its analogs may also affect brain functions other than those related to endocrine and metabolic regulation.

Ghrelin that is produced both peripherally and centrally is thought to be capable of changing energy balance by modulating hypothalamic and brainstem circuitry[1,3,8]. In particular, the mediobasal and paraventricular hypothalamic melanocortin system was found to be targeted and modulated by ghrelin. In slice preparations, orexigenic agouti related peptide (AgRP)-expressing cells are activated by ghrelin, whereas anorexigenic pro-opiomelanocortin (POMC) neurons are inhibited by it[8]. In addition to the acute electrophysiological effects of ghrelin on these neurons, peripheral ghrelin administration has also been shown to rapidly reorganize the synaptic inputs of POMC neurons[9]. The resultant synaptic rewiring of POMC neurons further promotes the suppression of these arcuate cells[9], which is consistent with the overall orexigenic influence of ghrelin.

Synaptic plasticity has traditionally been associated with higher brain functions, including learning and memory processing. In particular, various forms of neuronal plasticity within the hippocampal formation are thought to underlie spatial learning and memory development. Growth hormone secretagogue receptors (also referred to as ghrelin receptors) were identified in the hippocampal formation even before ghrelin and its functions were revealed[6]. This information, together with our observation that ghrelin modulates morphological synaptic plasticity of the hypothalamus[9], raised the question of whether ghrelin would bind and enter the hippocampus, and whether its presence there indicates that it has a physiologic role in altering neuronal morphology and associated hippocampal functions. Our results show that circulating ghrelin can reach the hippocampal formation, where it alters neuronal morphology, generation of long-term potentiation (LTP) and behavioral outputs.

[1]Department of Obstetrics and Gynecology and Reproductive Sciences, Yale University School of Medicine, New Haven, Connecticut 06520, USA. [2]Geriatric Research Education and Clinical Center (GRECC), VA Medical Center, St. Louis, Missouri 63106, USA. [3]Department of Internal Medicine, Division of Geriatric Medicine, St. Louis University School of Medicine, St. Louis, Missouri 63106, USA. [4]Department of Psychiatry, University of Cincinnati, Cincinnati, Ohio 45237, USA. [5]Department of Internal Medicine, Yale University School of Medicine, New Haven, Connecticut 06520, USA. [6]Department of Molecular Genetics, Howard Hughes Medical Institute, Rockefeller University, New York, New York 10021, USA. [7]Department of Neurology, Washington University School of Medicine, St. Louis, Missouri 63110, USA. [8]Regeneron Pharmaceuticals Inc., Tarrytown, New York 10591, USA. [9]Department of Neurobiology and [10]Section of Comparative Medicine, Yale University School of Medicine, New Haven, Connecticut 06520, USA. Correspondence should be addressed to T.L.H. (tamas.horvath@yale.edu).

Received 19 December 2005; accepted 31 January 2006; published online 19 February 2006; doi:10.1038/nn1656

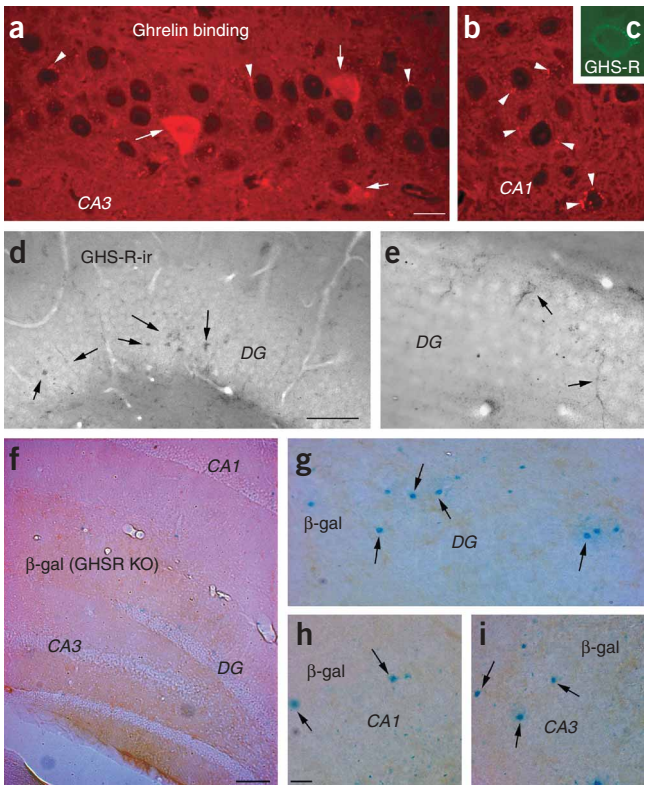

Figure 1 Ghrelin binding in the hippocampus. (**a**,**b**) Fluorescent images of ghrelin binding in the hippocampal formation. Biotinylated ghrelin (red fluorescence) was found in scattered cell bodies (white arrows) of the principal layer of the hippocampal formation (**a**) and in association with bouton-like structures (white arrowheads) surrounding putative pyramidal cells (**a** and **b**). Scale bar in **a** represents 10 μm for **a**, **b** and **c**. (**c**–**e**) GHS-R immunoreactivity was associated with cells of the hippocampus (**c**–**e**; arrows in **d** and **e**). The distribution of GHS-R immunoreactivity corresponded with the results of the binding assay (**a** and **b**). High-power magnification of GHS-R immunolabeling revealed punctate labeling (**c**), which was similar to the appearance of bitotinylated ghrelin binding (**b**). Scale bars represent 100 μm and 20 μm for panels **d** and **e**, respectively. (**f**–**i**) β-gal labeling of hippocampal slices taken from GHS-R knockout animals that was generated using the *lacZ* reporter gene. β-gal labeled cells (arrows) were most visible, even at low magnification, in the dentate gyrus (**f** and **g**), but scattered cells were also found in the CA1 (**h**) and CA3 (**i**) subfields of the hippocampal formation. The distribution of β-gal-positive cells was similar to that revealed by either the binding assay or immunocytochemistry. Scale bars represent 100 μm for panel **f** and 10 μm for panels **g**–**i**.

RESULTS

Ghrelin binding and receptors in the hippocampus

Robust extra-hypothalamic ghrelin binding sites, in addition to those already reported in the cerebral cortex[8], were identified in the hippocampal formation (**Fig. 1a**,**b**). The distribution of labeled cells and processes suggests binding of ghrelin predominantly in the processes of hippocampal neurons (**Fig. 1a**,**b**). Labeled cells appeared in the dentate gyrus, as well as in the CA3 and CA1 regions of the hippocampus. To confirm that GHS-Rs are present in these areas, we analyzed GHS-R immunolabeling in wild-type mice as well as β-galactosidase (β-gal) expression in the hippocampal formation of GHS-R knockout animals. These animals express β-gal instead of GHS-R in the same cells, since they were generated by inserting the reporter gene *lacZ* driven by the GHS-R promoter in place of the gene that encodes GHS-R (see Methods for further details). All three approaches consistently confirmed the presence of GHS-R in the dentate gyrus and the CA3 and CA1 fields of the hippocampal formation, with the greatest number of labeled cells seen in the dentate gyrus (**Fig. 1c–i**).

Peripheral ghrelin enters the hippocampus

Ghrelin passively crosses the blood-brain barrier from the periphery[10]. To determine whether peripheral ghrelin can enter the hippocampus as well, we analyzed the presence of radiolabeled human ghrelin in various parts of the mouse brain after peripheral injection (see Methods for details). The brain/serum ratios of ghrelin were statistically significant for all brain regions analyzed ($P < 0.05$). The hypothalamus exhibited the third highest uptake, with a K_i (see Methods) of 2.3 ± 0.5 μl/g●min (the olfactory bulb and occipital cortex had the highest K_i values: 2.8 and 3.0 μl/g●min, respectively). The hippocampus had an intermediate uptake of 1.2 ± 0.3 μl/g●min, similar to the uptake for whole brain of 1.1 μl/g●min (**Fig. 2**). An analysis of variance (ANOVA) showed that the K_is for these regions differed significantly ($F_{2,35} = 7.6$, $P < 0.005$) and the Newman-Keuls multiple comparison test showed that hypothalamic uptake was greater than that of the hippocampus ($P < 0.05$). A dose of 10 μg/mouse of unlabeled ghrelin inhibited uptake into the hypothalamus and hippocampus was used to confirm that ghrelin uptake is saturable (**Fig. 2**).

CA1 spine synapse number is altered by ghrelin

Peripheral ghrelin administration was recently found to rapidly re-arrange the synaptic organization of hypothalamic anorexigenic neurons[9]. To reveal whether such rapid synaptic remodeling may also occur in the hippocampus in response to changes in circulating ghrelin levels, we assessed the density of axo-spinal synapses in the CA1 subfield of the hippocampus using electron microscopic unbiased stereology. We analyzed hippocampal tissue from animals that received peripheral administration of either synthetic ghrelin ($n = 6$) or saline ($n = 6$) as described previously[9], at a dosage that induced transient elevation in food intake and changes in the synaptology of arcuate nucleus melanocortin cells[9] (see Methods for details).

Spine synapse density in the CA1 subfield of the hippocampal formation was significantly higher in ghrelin-treated animals compared to vehicle-treated controls (0.455 ± 0.025 vs. 0.345 ± 0.011 spine

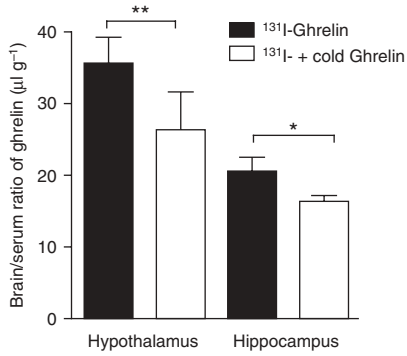

Figure 2 Peripherally administered ghrelin enters the hippocampus. The relation between brain/serum ratios of radiolabeled ghrelin was statistically significant for both the hypothalamus and hippocampus (filled bars). Injection of 10 μg/mouse of unlabeled ghrelin significantly decreased the uptake of ^{131}I-labeled ghrelin into the hypothalamus and hippocampus (empty bars), thus confirming the specificity of ghrelin uptake.

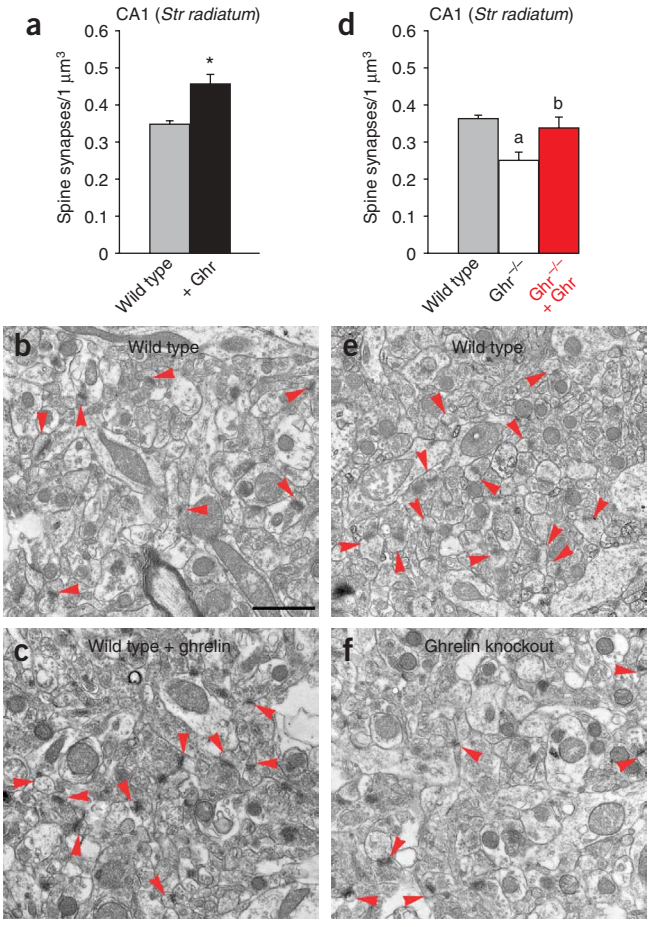

Figure 3 Effect of ghrelin on hippocampal spine synapse density. (**a**–**c**) Peripheral ghrelin administration to wild-type mice resulted in an increased density of spine synapses in the stratum radiatum of the hippocampal CA1 subfield (**d**, a: $^*P < 0.05$). A representative electron micrograph showing spine synapses (red arrowheads) in control wild-type (**b**) and ghrelin-treated wild-type animals (**c**). (**d**–**f**) Ghrelin knockout animals exhibited a lower density of hippocampal spine synapses than wild-type littermates (b: $^*P < 0.05$), however, ghrelin administration to these transgenic animals elevated spine synapse number ($P < 0.05$) making this parameter indistinguishable from wild-type values. A representative electron micrograph showing spine synapses (red arrowheads) in wild-type (**e**) and ghrelin knockout animals (**f**). Scale bar in **b** represents 1 µm for panels **b**, **c**, **e** and **f**.

synapses/µm^3; $P < 0.01$; **Fig. 3a**–**c**), whereas the volume and cellular density of the hippocampus did not differ (data not shown). To address whether endogenous ghrelin also controls spine synapse density, we assessed the same parameters in the CA1 region of ghrelin knockout mice (*Ghrl*$^{-/-}$, $n = 5$)[11] and their wild-type littermates ($n = 5$). We detected significantly lower numbers of dendritic spines in *Ghrl*$^{-/-}$ compared to wild-type littermates (0.25 ± 0.02 vs. 0.36 ± 0.01 spine synapses/µm^3; $P < 0.001$; **Fig. 3d**–**f**). To determine whether exogenous ghrelin can alter spine synapse density in the CA1 region of *Ghrl*$^{-/-}$ animals, we assessed this parameter in knockouts and their littermates ($n = 5$ for each group) following the paradigm for ghrelin administration of wild types (see above and ref. 7). This treatment resulted in a shift in spine synapse density of *Ghrl*$^{-/-}$ animals toward the wild-type values (ghrelin-treated *Ghrl*$^{-/-}$, 0.332 ± 0.02; saline-treated *Ghrl*$^{-/-}$, 0.243+0.018; $P < 0.01$; **Fig. 3d**).

Ghrelin's effect on LTP

To determine whether ghrelin may also affect other types of synaptic plasticity, we tested whether ghrelin affects the generation of LTP in slice preparations. The excitatory postsynaptic potential (EPSP) slope at 35–40 min after 10-Hz stimulation was 124 ± 3.3% ($n = 12$ slices, 10 mice) in artificial cerebrospinal fluid (ACSF)-treated slices and 148.0 ± 3.8 ($n = 10$ slices, 9 mice) in the ghrelin-treated group ($P < 0.05$; **Fig. 4**), revealing a significant ghrelin-induced change in hippocampal LTP. There was no significant difference after theta burst stimuli at 35–40 min: the EPSP slope was 171.6 ± 3.3% in ACSF ($n = 11$ slices, 10 mice) and 169.5 ± 4.5 in the ghrelin group (11 slices, 10 mice).

Ghrelin's effect on learning and memory processes

To determine the effect of ghrelin and a GHS-R agonist, LY444711 (ref. 12), on spatial memory, we started by studying rats in a spontaneous alternation plus-maze task. This plus-maze task and spontaneous alternation in general have been used extensively before[13–17]. This task is designed to impose a significant memory load, and the hippocampal dependence of the task has been previously demonstrated[14,16–24]. Before testing, animals were given a single subcutaneous injection of ghrelin ($n = 6$; 10 µg/kg, in saline), the ghrelin mimetic LY444711 ($n = 6$; 5 mg/kg, in saline with 5% DMSO) or a matched volume of the respective vehicles ($n = 6$ for saline control group and $n = 6$ for saline with 5% DMSO group). Both ghrelin and LY444711 produced a marked improvement of alternation performance over control animals (**Fig. 5a**). The performance of animals in the two control groups was similar ($t_{10} = 1.12$, $P = 0.29$), as was the performance in the two drug-treatment groups ($t_{10} = 0.15$, $P = 0.88$). Such acute and peripheral drug treatment did not significantly alter general ambulatory activity, as measured by the number of maze arms entered ($t_{10} = 0.75$ and 0.78, respectively).

To further analyze ghrelin's effect on memory, we studied the post-training influence of intracerebroventricular (i.c.v.) ghrelin administration on retention performance in T-maze foot-shock avoidance and step-down passive avoidance tasks in mice (**Fig. 5b**,**c**). Mice were prepared for i.c.v. injection 48 h before training. Immediately after training, the mice received a 2-µl injection of ghrelin ($n = 10$/group; 0, 50, 75, 100, 150, 200 ng per injection) and retention performance was tested 1 week later. Ghrelin improved retention ($F_{6,63} = 9.39$, $P < 0.001$; **Fig. 5b**) when administered immediately after training, suggesting an effect on consolidation. In a

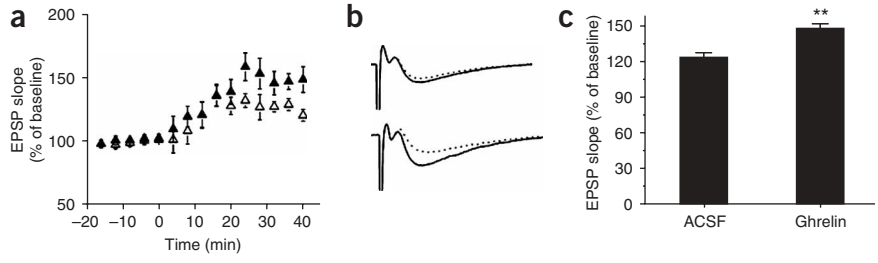

Figure 4 Ghrelin promotes LTP generation. (**a**–**c**) We tested the effect of ghrelin on generation of LTP in slice preparations. The EPSP slope at 35–40 min after 10 Hz stimulation was 124 ± 3.3 ($n = 12$ slices, 10 mice) in ACSF-treated slices and 148.0 ± 3.8 ($n = 10$ slices, 9 mice) in the ghrelin-treated group ($P < 0.05$), revealing a significant ghrelin induced change in hippocampal LTP.

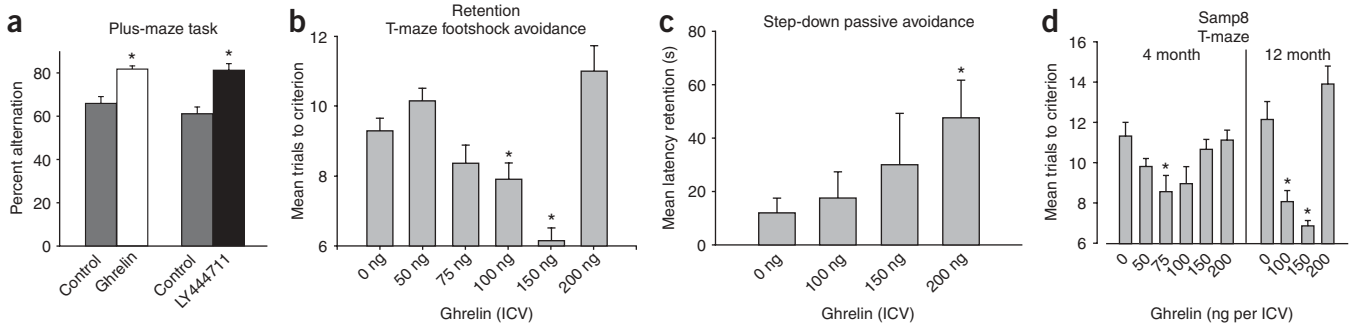

Figure 5 Effects of ghrelin treatment on learning and memory performance. Bar graphs showing enhanced performance of animals after ghrelin or ghrelin analog treatment in the plus maze task (**a**, $^*P < 0.05$), after ghrelin treatment in the T-maze foot shock avoidance (**b**, $^*P < 0.05$) and step-down passive avoidance (**c**, $^*P < 0.05$) tasks. (**d**) Ghrelin also enhanced the performance of SAMP8 mice in the T maze at 4 months of age ($^*P < 0.05$) as well as at 12 months ($^*P < 0.05$). At 12 months of age these animals showed Alzheimer disease-like symptoms, and a higher dose of ghrelin was required to elicit the same response in these older animals.

one-trial step-down passive avoidance test, another set of mice were administered ghrelin ($n = 10$/group; 0, 100, 150 and 200 ng per 2 μl) immediately after training and retention was tested 24 h later. Ghrelin improved retention in this test of memory as well ($F_{3,36} = 4.90$, $P < 0.005$; **Fig. 5c**). In SAMP8 mice, the phenotype of which mimics pathological and cognitive signs of Alzheimer disease[25], ghrelin improved retention of T-maze foot shock avoidance in 12-month old ($F_{4,49} = 3.45$, $P < 0.01$) and 14-month old ($F_{3,35} = 13.07$, $P < 0.001$; **Fig. 5d**) mice. SAMP8 mice have an age-related increase in beta amyloid, which corresponds with their age-related impairment in learning and memory. By 12 months of age, these mice are impaired in T-maze foot-shock avoidance (**Fig. 5d**). Ghrelin improved memory in all cases. Notably, in all T-maze tests, a U-shaped dose-response curve was observed. This may relate to a concentration-dependent spread of ghrelin to the various brain sites that contain ghrelin receptors that either promote or inhibit performance in T-maze foot shock avoidance.

To test whether endogenous ghrelin has a physiologic role in improving learning and memory performance, we measured how ghrelin-null mice performed in a spatial-dependent version of the novel object recognition (NOR) test, which reflects memory that is dependent upon the hippocampus[26,27]. During training, mice were first allowed to explore two novel objects (A and B) in a test chamber for 5 min. Total exploration time was similar between both *Ghrl*$^{-/-}$ and wild-type animals (data not shown), and both genotypes spent similar amounts of time at each object (A and B). After a 4-h delay, one of the original objects was replaced with a new object (C), and the spatial location and exploration time was again measured. Wild-type mice exhibited increased exploration time of the novel object (C) (**Fig. 6a**, left bars), indicating memory of the previously explored objects (A or B). Ghrelin-deficient mice, however (**Fig. 6b**, right bars), did not exhibit increased exploration time of the novel object (C), suggesting impairment in their memory of the previous objects, but this functional deficiency disappeared rapidly upon ghrelin replacement therapy administered by subcutaneous mini-pumps (**Fig. 6b**).

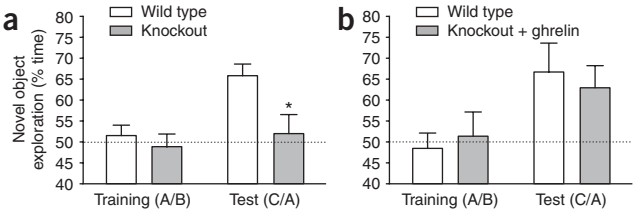

Figure 6 Ghrelin's effect on memory performance of *Ghr*$^{-/-}$ mice. (**a**,**b**) Bar graphs demonstrating that ghrelin knockout mice exhibit decreased memory performance relative to wild-type mice. Wild-type, but not ghrelin knockout, mice showed an increased orientation to novel objects in the spatial NOR test (**a**, $^*P < 0.05$). This difference was abolished by 14 d of ghrelin replacement (**b**) to the knockouts. Ghrelin knockout mice treated with vehicle again showed chance performance (data not shown).

DISCUSSION

Ghrelin was originally discovered as a regulator of growth hormone release[1], and it was subsequently identified as an appetite-stimulating adipogenic hormone[2]. Ghrelin is secreted from the stomach when the stomach is empty[28]. Thus, the major emphasis of ghrelin research has been on possible roles for ghrelin in meal initiation[29] and energy homeostasis in general[30,31]. However, the current study provides evidence that ghrelin that originates in the periphery may also control higher brain functions and may represent a molecular link between learning capabilities and energy metabolism. Our results revealed that circulating ghrelin enters the hippocampal formation, where it binds to neurons. Ghrelin receptors are expressed in neurons of the hippocampus, and ghrelin promotes the formation of spine synapses in the stratum radiatum of the CA1 subfield of the hippocampal formation. In addition, ghrelin promotes LTP generation in hippocampal slice preparations. The spine synapse number of CA1 pyramidal neurons and LTP are known to have a positive correlation with spatial memory and learning[32]. The elevated ghrelin levels in association with changes in synapse number were paralleled by enhanced performance of animals in a variety of behavioral tests that are known to be dependent, at least in part, on the hippocampus. In line with these data, ghrelin knockout animals had a smaller number of spine synapses in the stratum radiatum and underperformed their wild-type littermates in novel object recognition tests. Ghrelin administration, however, rapidly restored this impairment in the ghrelin knockout mice, indicating that this stomach hormone and neuropeptide governs neuronal morphology of brain areas known to be responsible for learning performance and memory formation. A similar relationship between altered hippocampal spine synapse morphology and spatial learning performance was also observed in response to the circulating gonadal hormone estradiol[33].

Ghrelin- or GHS-R null mutant animals show no obvious metabolic phenotype[11,34] while on a standard diet, though it was recently reported that they show resistance to diet-induced obesity[11,34]. Thus,

there is reason to believe that ghrelin (unlike leptin) may not be a critical regulator of homeostatic energy balance. In fact, one of the first reported phenotypes of ghrelin knockout animals was our observation of a significant impairment of these animals in the NOR test. This suggests that ghrelin may be more important for the regulation of higher brain functions that are dependent upon metabolic status rather than for energy metabolism *per se*. This may not be all that surprising given that a great number of cognitive tests on laboratory rodents and nonhuman primates are carried out after food deprivation or fasting, metabolic states that are paralleled by elevated levels of circulating ghrelin. The notion that spatial learning and unfocused attention would be enhanced during fasting is also in line with the necessity of an animal that is in negative energy balance to identify and locate energy sources in order to survive. It has also been demonstrated that diets high in saturated fatty acids, which promote obesity, impair some forms of hippocampus-dependent memory formation in rodents[35]. Because both aging and obesity are associated with low ghrelin levels[36,37], and the progression of dementias such as Alzheimer disease are promoted by age and obesity[38], our findings raise the possibility that ghrelin supplementation may attenuate the development of these neurological pathologies. In line with these findings are our results on SAMP8 mice, which exhibit late-onset behavioral declines similar to Alzheimer disease patients[25]. These mice clearly benefited from ghrelin administration in that their behavioral performance was restored.

The precise molecular mechanisms that underlie the effects of ghrelin on hippocampal function remain to be elucidated. Additionally, consideration must be given to the fact that the behavioral tasks used in the present study, while diverse, are not solely dependent upon hippocampal function. It is also very likely that ghrelin exerts its effect on higher brain functions not only through direct action in the hippocampus, but also through other telencephalic and basal forebrain sites as well. This idea is in line with earlier findings of ghrelin binding to cortical cells[8]. Another area of inquiry is whether the downstream signaling systems that mediate the effects of ghrelin on food intake and body weight regulation are the same as those that mediate the effects on learning and memory processes in the hippocampus. If they are the same, this may present challenges relevant to the use of drugs in the clinic that target the ghrelin system for the treatment of obesity or diabetes. For example, one possible side effect of ghrelin inhibition might be reductions in hippocampal function and/or neuronal plasticity, which depend upon ghrelin signaling. Likewise, the dual effects of ghrelin and other hormones present challenges for developing treatments for cognitive disorders. Because ghrelin may increase food intake and body adiposity, the use of the hormone itself in the treatment of cognitive impairment might also be associated with the development of obesity. Nonetheless, a fuller understanding of the specific mechanisms that mediate these effects of ghrelin may shed light on novel strategies that elicit only one of the desired effects, whether that be reduced body weight or enhanced cognitive function.

In summary, the present observations support the idea that peripheral metabolic signals, which have predominantly been associated with endocrine and metabolic regulation thus far, may have a profound influence on higher brain functions. Our results show that peripheral ghrelin has a robust impact on hippocampal synaptology. In parallel, systemic administration of ghrelin or its analogs enhance learning and memory, whereas the absence of ghrelin due to targeted gene disruption causes impairment of these functions. Thus, orally active GHS analogs may offer a potential treatment for impaired learning and memory processing, which occurs in association with aging and neurological disorders such as Alzheimer disease.

METHODS

All procedures described below have been approved by the Institutional Animal Care and Use Committees of Yale University, St. Louis University, University of Cincinnati and Regeneron Pharmaceuticals Inc.

Animals. For anatomical analyses and for the novel object recognition test, wild-type (c57/Bl6) and ghrelin-deficient mice were obtained from Regeneron Pharmaceuticals and were generated as previously described[39]. Some anatomical studies were also carried out on GHSR knockout animals (see below for details. For the plus-maze task memory testing, male Sprague-Dawley rats were used (Harlan, Indianapolis).

For the T-Maze footshock tests, step-down passive avoidance tests and for the analysis of ghrelin's ability to enter the hippocampus, CD-1 male mice (4 months of age) were studied. This colony had been maintained for 2 years as an outbred strain obtained from Charles River Breeding Laboratories (Wilmington, Massachusetts). SAMP8 male mice, 4 and 12 months of age, were also analyzed in T-maze footshock avoidance tests. These animals were obtained from a breeding colony at St. Louis University. This colony had been maintained for 15 years as an inbred strain from siblings provided by T. Takeda (Kyoto University, Japan).

For all animals, water and food were available *ad libitum*. All subjects were experimentally naive. All rodents were on a 12 h light: 12 h dark cycle with lights on at 6 a.m.

Ghrelin and ghrelin receptor knockout animals. We used high-throughput homologous recombination technology[34,39,40] to generate these animals. Briefly, bacterial artificial chromosome (BAC) for GHSR was isolated and targeting vectors, in which the coding region of the *Ghsr* locus (from ATG initiation codon to near the termination codon) was precisely deleted and replaced with an in-frame *lacZ* reporter gene and neomycin selectable marker, were electroporated into embryonic stem cells. Correctly targeted embryonic stem cells, as well as eventual heterozygote and homozygous mice derived from these cells, were identified by a real-time PCR–based loss-of-native-allele assay as previously described[40]. After germline transmission was established, F1 heterozygous mice were backcrossed to C57BL6/J to generate N3 breeding heterozygote pairs that were used to generate the homozygous $Ghsr^{+/+}$ and $Ghsr^{-/-}$ mice that were used in these experiments. All experiments reported were conducted on N3F2 littermates that were housed under 12 h of light per day in a temperature-controlled environment. The deletion of *Ghsr* was also confirmed by the absence of exogenous ghrelin-induced feeding response (M.S., unpublished data). For ghrelin replacement, ghrelin knockout mice were implanted with Alzet minipumps which delivered subcutaneous ghrelin (2.4 μmol kg^{-1} per d; $n = 6$) or vehicle ($n = 6$) for 14 d. β-galactosidase (β-gal), which is the product of the *lacZ* gene, was visualized as described previously[39].

Ghrelin binding assay. The ghrelin binding assay on coronal rat hippocampal slices was carried out as detailed recently[8]. Tissues were fixed overnight in zinc-buffered formalin and then transferred to 70% ethanol prior to processing through paraffin. Five-micron sections were prepared and placed on positively charged slides. The slides were then baked overnight at 60 °C in an oven and then deparaffinized in xylene and rehydrated through graded alcohols to water. Antigen retrieval was performed by immersing the slides in target retrieval solution (Dako Corp.) for 20 min at 90 °C (in a water bath), cooling them at room temperature (22 °C) for 10 min, washing them in water and then proceeding with immunostaining. All subsequent staining steps were performed on the Dako Autoimmunostainer; incubations were done at room temperature and Tris-buffered saline plus 0.05% Tween 20, pH 7.4 (TBS, Dako Corp.) was used for all washes and diluents. Thorough washing was performed after each incubation. Slides were blocked with protein blocking solution (Dako) for 25 min; after washing, 10 μg ml^{-1} of biotinylated ghrelin (Eli Lilly) was then added to the slides and incubated for 60 min. A streptavidin-horseradish peroxidase kit (Dako LSAB2) was used along with Alexa 568 dye (red fluorescence) to detect the bound avidin-biotin-ghrelin complexes. The slides were briefly counterstained with hematoxylin, removed from the autostainer and dehydrated through graded alcohols to xylene. The slides were coverslipped with a permanent mounting medium and analyzed with a

fluorescence microscope. Both unlabeled ghrelin and biotin were used as negative controls in which case no specific labeling was detected. For cold ghrelin competition with biotinylated ghrelin, we also used a modified binding assay on fresh, unfixed hippocampal slices. In this case, saline-perfused brains were removed, sectioned and immediately reacted with biotinylated ghrelin (1 μM; Phoenix Pharmaceuticals) alone or in combination with an equal amount of unlabeled (cold) ghrelin (1 μM; Phoenix Pharmaceuticals) for 20 min at 4 °C. Subsequently, sections were fixed with 4% paraformaldehyde and reacted with avidin-Texas red and analyzed.

GHS-R immunocytochemistry. A separate set of 50-μm vibratome sections cut across the hippocampal formation of fixed brains was processed for immunocytochemistry using rabbit antisera raised against the Cys (330–366) portion of the human GHS-R1a sequence (Phoenix Pharmaceuticals). Control sections were incubated in antibody preabsorbed with the human GHS-R1a protein (20 mg ml^{-1}), or without primary antiserum for negative controls. Sections were washed several times and reacted with 1% H_2O_2 in 0.1M phosphate buffer (PB) for 30 min. Following several washes, sections were incubated in 10% sucrose for 2 h for cryoprotection, and then snap frozen in liquid nitrogen and thawed. After washing several times, slices were incubated in blocking serum (2% normal horse serum in 0.1 M PB) for 1 h, and then incubated in primary antibody (1:1,000 in blocking solution) for 72 h at 4 °C. After several washes with PB, sections were incubated in biotinylated donkey anti rabbit (1:250, Jackson Laboratories) for 2 h at room temperature, washed, and incubated in avidin biotin peroxidase complex (ABC) (Vector Labs). Following washing, sections were developed with nickel-intensified diaminobenzidine, mounted and coverslipped in Depex mounting medium (Electron Microscopy Sciences). No staining was observed in brain tissue sections from GHS-R knockout mice (data not shown).

β-gal labeling. *GHS-R* knockout mice were perfused with 4% paraformaldehyde. Brains were sectioned with a vibratome (40 μm) and washed with phosphate-buffered saline (PBS: 137 mM NaCl, 2.7 mM KCl, 8 mM Na_2HPO_4, 2.6 mM KH_2PO_4) four times. Sections containing the hippocampus were then quickly rinsed once in cold PBS plus 2 mM $MgCl_2$ and incubated in the above solution for 10 min at 4 °C. Permeabilization was performed by incubation in cold PBS with detergent (0.01% sodium desoxycholate and 0.02% NP40) for 10 min. Sections were then incubated overnight at 37 °C in the staining solution containing 25 mM $K_3Fe(CN)_6$, 25 mM $K_4Fe(CN)_6$, 2 mM $MgCl_2$ in PBS and 1 mg ml^{-1} of X-Gal.

Analysis of ghrelin entrance into the hippocampus. Human ghrelin was radioactively labeled with ^{131}I and purified (I-Ghr) as previously described[10]. CD-1 male mice (8 weeks old) were anesthetized with urethane and I-Ghr was injected into the left jugular vein. Arterial serum was obtained from the abdominal aorta between 1 and 10 min after the injection of I-Ghr, and the brain, including the olfactory bulbs, was harvested. Between the collection of the blood and the brain, the jugular veins were severed and the vascular space of the brain was washed out by perfusing 20 ml of saline through the left ventricle of the heart. The brain was dissected into ten regions as previously described[41]. Multiple time regression analysis[25,35] was used to calculate the blood to brain unidirectional influx rate (K_i) and its error term for each brain region. The brain/serum ratios were plotted against their respective exposure times (T_{Exp}). T_{Exp} was calculated using the following formula: $T_{Exp} = [\int_0^t Cp(\tau)d\tau]/Cp_t$, where Cp is the level of radioactivity in serum and Cp_t is the level of radioactivity in serum at time t. T_{Exp} corrects for the clearance of peptide from the blood. K_i with its error term is measured as the slope for the linear portion of the relation between the brain/serum ratios and T_{Exp} and the y-intercept of the linearity measures V_i, the distribution volume in brain at $t = 0$, so that the equation describing the linear portion of the relation between brain/serum ratios and T_{Exp} is: Brain/serum ratio $= K_i(T_{Exp}) + V_i$.

To determine whether I-Ghr was crossing into brain regions by a saturable process, mice received intravenous (i.v.) injections of I-Ghr with or without 10 ϒ g per mouse of unlabeled ghrelin. Arterial blood and brains were collected 5 min after the i.v. injection and the brains were dissected as described above. Results were expressed as brain/serum ratios with their standard errors.

Statistics. The Prism 4.0 program (GraphPad) was used to calculate K_i with its error term. K_i values were compared by one-way ANOVA. Means between two groups were compared by Student's t-test and between more than two groups by ANOVA.

Synapse counts. Wild-type mice were treated by intraperitoneal (i.p.) injection of 100 μl of 0.1 μg μl^{-1} ghrelin solution dissolved in PBS or with PBS alone. Injections took place at 9 a.m. and 3 p.m. on four consecutive days. Animals (8-week-old male mice) were perfused between 30 min and 1 h after the last injection on the fourth day. In another set of ghrelin knockout animals, ghrelin was replaced using an Alzet minipump, which provided 3.5 mg kg^{-1} per d of ghrelin dissolved in saline or the vehicle only.

Animals were killed under deep ether anesthesia by transcardial perfusion of heparinized saline followed by a fixative containing 4% paraformaldehyde and 0.1% glutaraldehyde in 0.1 M phosphate buffer (pH 7.35). The brains were removed and postfixed overnight in the same fixative without glutaraldehyde. Then the hippocampi were dissected out and 100-μm vibratome sections were cut perpendicular to the longitudinal axis of the hippocampus. Approximately 90 vibratome sections were divided into ten portions using systematic, uniformly random sampling. Sections were postfixed in 1% osmium tetroxide (40 min), dehydrated in ethanol (the 70% ethanol contained 1% uranyl acetate; 40 min) and flat-embedded in Araldite between slides and coverslips. In each embedded vibratome section, a sampling area was randomly selected from the stratum radiatum of the CA1 region. Spine synapse density was calculated in all animal groups according to our standard protocol using unbiased stereological methods. To assess possible changes in the volume of the tissue, a correction factor was calculated assuming that the hormonal treatments did not alter the total number of pyramidal cells. In all hippocampi, six or seven dissector pairs (pairs of adjacent 2-μm toluidine blue–stained semithin sections mounted on slides) were analyzed. The pyramidal cell density value (D) was calculated using a formula: $D = N/sT$, where N is the mean dissector score across all sampling windows, T is the thickness of the sections (2 μm) and s stands for the length of the window. Based on these values, a dimensionless volume correction factor k_v was introduced: $k_v = D/D_1$, where D_1 is the main density across the groups of hippocampi. Thereafter, using the toluidine blue–stained semithin sections as guides, each block was trimmed to contain the same area, located between the middle and distal portion of the stratum radiatum. Pairs of consecutive serial ultrathin sections ('reference' and 'look-up') were cut from the vibratome sections taken from all parts of the hippocampus along its longitudinal axis. The section pairs were collected on Formvar-coated single-slot grids. Subsequently, digitized images were taken at a magnification of 11,000× in a Tecnai 12 transmission electron microscope furnished with an AMT Advantage 4.00 HR/HR-B CCD camera system. Identical regions in reference and look-up sections were identified using landmarks (myelinated fibers, large dendrites or blood vessels) that did not change appreciably between neighboring sections because of their size. Areas occupied by potentially interfering structures were subtracted using the NIH Scion image-processing software. To obtain a comparable measure of synaptic numbers, unbiased for possible changes in synaptic size, the dissector technique was used. Digitized electron micrographs were printed out and coded, and the code was not broken until the analysis was completed. Only those spine synapses that were present in one of the sections were counted (example in **Supplementary Figure 1** online). To increase the efficiency of counting, the analysis was performed treating each reference section as a look-up section, and vice versa. The density of spine synapses of pyramidal cell dendrites was calculated with the help of a reference grid superimposed on the electron microscopic prints. The dissector volume (volume of reference) was the unit area of the reference grid multiplied by the distance between the upper faces of the reference and look-up sections. Section thickness (average, 0.075 μm) was determined using the electron scattering technique. The measured synaptic density values were divided by the volume correction factor k_v. This correction provided a synaptic density estimate normalized with respect to the density of pyramidal cells and also accounted for possible changes in hippocampal volume.

At least five neuropil fields (each 80 μm^2) were photographed on each electron microscopic grid. With at least three grids (containing a minimum of two pairs of consecutive, serial ultrathin sections) prepared from each vibratome section (cut from the three portions of the hippocampus along its

longitudinal axis), each animal provided at least $3 \times 3 \times 5 \times 2 = 90$ neuropil fields for evaluation, corresponding to a total section area of 7,200 μm^2 (a total neuropil volume of 540 μm^3) per animal. The mean synapse densities for each animal were determined blind, independently by two different investigators and the results were cross-checked to preclude systematic analytical errors. Individual mean synapse densities for each animal were used to calculate means and standard errors for overall synapse density, in each experimental group. In our studies, $n = 1$ represents the mean data collected from one animal. Results were analyzed by means of an initial two-way ANOVA, followed by the Scheffe test for comparison of individual group means.

LTP analysis. Hippocampal slice preparation was done as previously described[42]. CD-1 mice were anesthetized with halothane and decapitated. The brain was quickly removed, cooled in ice-cold ACSF containing 124 mM NaCl, 5 mM KCl, 2.5 mM $CaCl_2$, 1.5 mM $MgCl_2$, 1.3 mM NaH_2PO_4, 22 mM $NaHCO_2$ and 10 mM glucose, and bubbled with 95% O_2/5% CO_2. The brain was mounted on a vibratome and 400-µm coronal sections containing the dorsal hippocampus were prepared in ice-cold ACSF. Sections were incubated in ACSF at room temperature (22 °C) at least one hour before the experiment. For the ghrelin group, the slice was incubated for 30 min in ghrelin (10^{-8} M), after which the slice was placed in the submersion recording chamber and constantly perfused with ACSF at roughly 5 ml/min at 30–31 °C.

Electrophysiology. Extracellular recordings were obtained from the stratum radiatum of the CA1 region of the hippocampus using glass electrodes filled with 2M NaCl (~5 MΩ DC resistance). Bipolar constant-current pulses (0.1–0.2 ms) were applied to the Schaffer collateral pathway to elicit excitatory postsynaptic potentials (EPSPs). We used the stimulus intensity that would evoke a 50% maximal amplitude EPSP, and was empirically determined for each slice. After ensuring a stable baseline response, 20 min of baseline EPSPs were acquired at 1-min intervals. In all experiments, baseline synaptic transmission was monitored for 20 min before stimulation with 10 Hz (200 pulse) or a series of four theta-burst stimuli (TBS) separated by 20-s intervals. The TBS were applied using the baseline stimulus intensity. A single theta burst stimulus consisted of a train of five pulses at 10-ms intervals, repeated ten times at 200-ms intervals (total of 50 pulses). Therefore, LTP induction consisted of a total of 200 pulses.

Spontaneous alternation plus-maze task. Twenty-four 3-month-old Sprague-Dawley male rats were used for memory testing. Animals were extensively handled for one week prior to testing. Thirty minutes prior to placement on the maze, animals received a single subcutaneous injection of either 0.25 ml ghrelin (10 µg/kg), ghrelin mimetic LY444711 (5 mg/kg) or an appropriate vehicle control. Animals were then placed into the center of the maze and allowed to explore freely for 20 min while arm entries were recorded. Performance scores were calculated as described previously[24].

T-maze footshock avoidance and step-down inhibitory avoidance paradigms. Octanoylated rat ghrelin (Phoenix Pharmaceuticals) was dissolved in saline and then injected i.c.v. in a volume of 2 µl. Drugs and concentrations were coded to prevent experimenter bias.

Forty-eight hours prior to testing, the mice were anesthetized with 2,2,2-Tribromoethanol, placed in a stereotaxic instrument, and the scalp was deflected. A unilateral hole was drilled 0.5 mm posterior to and 1.0 mm to the right of Bregma, to an injection depth of 2.0 mm into the third ventricle. Immediately after training, the mice were again placed under light anesthesia and injected with 2.0 µl of saline (i.c.v.) with or without ghrelin. The injection was delivered over 30 s through a 30 gauge needle, which was attached to a 10-µl syringe. After the injection, the scalp was closed and the mice were returned to their cages. The injection sites were confirmed histologically.

The T-maze footshock avoidance apparatus, training and testing procedures have been previously described[43]. The maze consisted of a black plastic start alley with a start box at one end and two goal boxes at the other. A stainless steel rod floor ran throughout the maze. The start box was separated from the start alley by a plastic guillotine door that prevented the mouse from moving down the alley until the training started. A training trial began when a mouse was placed into the start box. The guillotine door was raised and the buzzer sounded simultaneously. After 5 s, footshock was applied. The goal box the mouse first entered on the first trial was designated as "incorrect." Footshock was continued until the mouse entered the other goal box, which on all subsequent trials was designated "correct" for that particular mouse. At the end of each trial, the mouse was removed from the goal box and returned to its home cage. A new trial began by placing the mouse in the start box, sounding the buzzer and raising the guillotine door. Footshock was applied 5 s later if the mouse did not leave the start box or failed to enter the correct goal box. Retention for either training condition was tested one week later by continuing the training until each mouse made five avoidances in six consecutive training trials. Mice were trained under weak training condition and used an inter-trial interval of 35 s, a door-bell type buzzer at 55dB as the conditioned stimulus warning of onset of foot shock at 0.35 mA (Coulbourn Instruments scrambled grid floor shocker model E13-08). The parameters for this training condition were set so that the control groups would have poor retention (mean trials to criterion between 9 and 10) so that we could detect drug-induced improvement of retention.

Two days after surgery, the mice began a step-down inhibitory training paradigm. The box was 55 cm × 55 cm × 20 cm with a stainless steel rod floor. A 2.5-cm high, 7.5-cm wide square platform was placed in the center of the apparatus. Mice were placed on the platform and their latency to step down, defined as placing all four paws on the floor, was measured. On stepping down, they received a 0.28 mA footshock for 2 s. One trial was given during training. During the test session, mice were placed on the platform, but no footshock was given when they stepped off. Retention was tested 24 h after training by placing the mouse on the platform and measuring latency to step down onto the grid. Retention test scores were expressed as test minus training step-down latency (ceiling, 180 s).

Object recognition memory tests. We measured performance of ghrelin knockout and wild-type mice on novel object recognition (NOR), a type of memory that is dependent on the hippocampus[26,27]. During training, mice were first allowed to explore two novel objects (A and B) in a 60 × 60 × 30 cm test chamber for 5 min. The time spent sniffing, touching and orienting to each object was recorded as exploration via the computer-controlled video capture software, Cleversys Topscan (Clever Sys). Total exploration time was similar between both genotypes, and mice spent similar amounts of time at each object (A and B). After a 24-h delay, one of the original objects was replaced with a new object (C) at a new location and exploration time was again measured. Testing time was also 5 minutes. Three months later, the ghrelin knockout mice were implanted with subcutaneous Alzet minipumps delivering either ghrelin (3.5 mg/kg per day ghrelin dissolved in saline, $n = 6$) or vehicle ($n = 6$). The spatial version of the NOR test was repeated in a novel context using different test objects. Results were expressed as means with their standard errors. The retention test scores were analyzed by one-way analysis of variance (ANOVA) for each group followed by Tukey's HSD *post-hoc* analysis. The n was 10 per group in each study.

Note: Supplementary information is available on the Nature Neuroscience website.

ACKNOWLEDGMENTS

The authors thank M. Shanabrough for technical assistance and editing of the manuscript and E. Borok for the electron microscopic analyses. This work was supported by grants from the US National Institutes of Health (DK60711, DK61619, NS40525, AG22880, DK70039, NS41725, DK7386, DK70039 and AA12743) and a VA Merit Review grant.

COMPETING INTERESTS STATEMENT

The authors declare that they have no competing financial interests.

Published online at http://www.nature.com/natureneuroscience/
Reprints and permissions information is available online at http://npg.nature.com/reprintsandpermissions/

1. Kojima, M., Hosoda, H., Date, Y., Nakazato, M. & Kangawa, K. Ghrelin is a growth-hormone-releasing acylated peptide from stomach. *Nature* **402**, 656–660 (1999).
2. Tschop, M., Smiley, D.L. & Heiman, M.L. Ghrelin induces adiposity in rodents. *Nature* **407**, 908–913 (2000).
3. van der Lely, A.J., Tschop, M., Heiman, M.L. & Ghigo, E. Biological, physiological, pathophysiological, and pharmacological aspects of ghrelin. *Endocr. Rev.* **25**, 426–457 (2004).

4. Horvath, T.L., Castañeda, T., Tang-Christensen, M., Pagotto, U. & Tschop, M.H. Ghrelin as a potential anti-obesity target. *Curr. Pharm. Des.* **9**, 1383–1395 (2003).
5. Kojima, M. & Kangawa, K. Ghrelin: structure and function. *Physiol. Rev.* **85**, 495–522 (2005).
6. Guan, X.M. *et al.* Distribution of mRNA encoding the growth hormone secretagogue receptor in brain and peripheral tissues. *Brain Res. Mol. Brain Res.* **48**, 23–29 (1997).
7. Mitchell, V. *et al.* Comparative distribution of mRNA encoding the growth hormone secretagogue-receptor (GHS-R) in *Microcebus murinus* (Primate, lemurian) and rat forebrain and pituitary. *J. Comp. Neurol.* **429**, 469–489 (2001).
8. Cowley, M.A. *et al.* The distribution and mechanism of action of ghrelin in the CNS demonstrates a novel hypothalamic circuit regulating energy homeostasis. *Neuron* **37**, 649–661 (2003).
9. Pinto, S. *et al.* Rapid rewiring of arcuate nucleus feeding circuits by leptin. *Science* **304**, 110–115 (2004).
10. Banks, W.A., Tschop, M., Robinson, S.M. & Heiman, M.L. Extent and direction of ghrelin transport across the blood-brain barrier is determined by its unique primary structure. *J. Pharmacol. Exp. Ther.* **302**, 822–827 (2002).
11. Wortley, K.E. *et al.* Absence of ghrelin protects against early-onset obesity. *J. Clin. Invest.* **115**, 3573–3578 (2005).
12. Seyler, D.E. *et al.* Effect of growth hormone secretagogue LY444711 on IGF-1, growth hormone, and cortisol levels in beagle dogs after one and seven daily oral doses. *Drug Dev. Res.* **49**, 260–265 (2000).
13. Sarter, M., Bodewitz, G. & Stephens, D.N. Attenuation of scopolamine-induced impairment of spontaneous alteration behaviour by antagonist but not inverse agonist and agonist beta-carbolines. *Psychopharmacology (Berl.)* **94**, 491–495 (1988).
14. Ragozzino, M.E., Parker, M.E. & Gold, P.E. Spontaneous alternation and inhibitory avoidance impairments with morphine injections into the medial septum. Attenuation by glucose administration. *Brain Res.* **597**, 241–249 (1992).
15. Ragozzino, M.E., Wenk, G.L. & Gold, P.E. Glucose attenuates a morphine-induced decrease in hippocampal acetylcholine output: an in vivo microdialysis study in rats. *Brain Res.* **655**, 77–82 (1994).
16. McNay, E.C., Fries, T.M. & Gold, P.E. Decreases in rat extracellular hippocampal glucose concentration associated with cognitive demand during a spatial task. *Proc. Natl. Acad. Sci. USA* **97**, 2881–2885 (2000).
17. McNay, E.C., McCarty, R.C. & Gold, P.E. Fluctuations in brain glucose concentration during behavioral testing: dissociations between brain areas and between brain and blood. *Neurobiol. Learn. Mem.* **75**, 325–337 (2001).
18. Bostock, E., Gallagher, M. & King, R.A. Effects of opioid microinjections into the medial septal area on spatial memory in rats. *Behav. Neurosci.* **102**, 643–652 (1988).
19. Ragozzino, M.E. & Gold, P.E. Glucose injections into the medial septum reverse the effects of intraseptal morphine infusions on hippocampal acetylcholine output and memory. *Neuroscience* **68**, 981–988 (1995).
20. Ragozzino, M.E., Hellems, K., Lennartz, R.C. & Gold, P.E. Pyruvate infusions into the septal area attenuate spontaneous alternation impairments induced by intraseptal morphine injections. *Behav. Neurosci.* **109**, 1074–1080 (1995).
21. Wan, R.Q., Givens, B.S. & Olton, D.S. Opioid modulation of working memory: intraseptal, but not intraamygdaloid, infusions of beta-endorphin impair performance in spatial alternation. *Neurobiol. Learn. Mem.* **63**, 74–86 (1995).
22. McNay, E.C. & Gold, P.E. Memory modulation across neural systems: intra-amygdala glucose reverses deficits caused by intraseptal morphine on a spatial task but not on an aversive task. *J. Neurosci.* **18**, 3853–3858 (1998).
23. Talley, C.P., Arankowsky-Sandoval, G., McCarty, R. & Gold, P.E. Attenuation of morphine-induced behavioral changes in rodents by D- and L-glucose. *Neurobiol. Learn. Mem.* **71**, 62–79 (1999).
24. McNay, E.C. & Gold, P.E. Age-related differences in hippocampal extracellular fluid glucose concentration during behavioral testing and following systemic glucose administration. *J. Gerontol. A Biol. Sci. Med. Sci.* **56**, B66–B71 (2001).
25. Morley, J.E. *et al.* Beta-amyloid precursor polypeptide in SAMP8 mice affects learning and memory. *Peptides* **21**, 1761–1767 (2000).
26. Myhrer, T. Exploratory behavior and reaction to novelty in rats with hippocampal perforant path systems disrupted. *Behav. Neurosci.* **102**, 356–362 (1988).
27. Reed, J.M. & Squire, L.R. Impaired recognition memory in patients with lesions limited to the hippocampal formation. *Behav. Neurosci.* **111**, 667–675 (1997).
28. van der Lely, A.J., Tschop, M., Heiman, M.L. & Ghigo, E. Biological, physiological, pathophysiological, and pharmacological aspects of ghrelin. *Endocr. Rev.* **25**, 426–457 (2004).
29. Cummings, D.E. *et al.* A preprandial rise in plasma ghrelin levels suggests a role in meal initiation in humans. *Diabetes* **50**, 1714–1719 (2001).
30. Horvath, T.L., Diano, S., Sotonyi, P., Heiman, M. & Tschop, M. Minireview: ghrelin and the regulation of energy balance–a hypothalamic perspective. *Endocrinology* **142**, 4163–4169 (2001).
31. Grove, K.L. & Cowley, M.A. Is ghrelin a signal for the development of metabolic systems? *J. Clin. Invest.* **115**, 3393–3397 (2005).
32. Burgess, N., Maguire, E.A. & O'Keefe, J. The human hippocampus and spatial and episodic memory. *Neuron* **35**, 625–641 (2002).
33. Li, C. *et al.* Estrogen alters hippocampal dendritic spine shape and enhances synaptic protein immunoreactivity and spatial memory in female mice. *Proc. Natl. Acad. Sci. USA* **101**, 2185–2190 (2004).
34. Zigman, J.M. *et al.* Mice lacking ghrelin receptors resist the development of diet-induced obesity. *J. Clin. Invest.* **115**, 3564–3572 (2005).
35. Wu, A., Molteni, R., Ying, Z. & Gomez-Pinilla, F. A saturated-fat diet aggravates the outcome of traumatic brain injury on hippocampal plasticity and cognitive function by reducing brain-derived neurotrophic factor. *Neuroscience* **119**, 365–375 (2003).
36. Rigamonti, A.E. *et al.* Plasma ghrelin concentrations in elderly subjects: comparison with anorexic and obese patients. *J. Endocrinol.* **175**, R1–R5 (2002).
37. Tschop, M. *et al.* Circulating ghrelin levels are decreased in human obesity. *Diabetes* **50**, 707–709 (2001).
38. Gustafson, D., Rothenberg, E., Blennow, K., Steen, B. & Skoog, I. An 18-year follow-up of overweight and risk of Alzheimer disease. *Arch. Intern. Med.* **163**, 1524–1528 (2003).
39. Wortley, K.E. *et al.* Genetic deletion of ghrelin does not decrease food intake but influences metabolic fuel preference. *Proc. Natl. Acad. Sci. USA* **101**, 8227–8232 (2004).
40. Valenzuela, D.M. *et al.* High-throughput engineering of the mouse genome coupled with high-resolution expression analysis. *Nat. Biotechnol.* **21**, 652–659 (2003).
41. Glowinski, J. & Iversen, L.L. Regional studies of catecholamines in the rat brain. I. The disposition of [^{3}H]norepinephrine, [^{3}H]dopamine and [^{3}H]dopa in various regions of the brain. *J. Neurochem.* **13**, 655–669 (1966).
42. Thio, L.L., Wong, M. & Yamada, K.A. Ketone bodies do not directly alter excitatory or inhibitory hippocampal synaptic transmission. *Neurology* **54**, 325–331 (2000).
43. Farr, S.A., Banks, W.A., La Scola, M.E., Flood, J.F. & Morley, J.E. Permanent and temporary inactivation of the hippocampus impairs T-maze footshock avoidance acquisition and retention. *Brain Res.* **872**, 242–249 (2000).